PERGAMON

International Journal of Solids and Structures 37 (2000) 2127–2150

INTERNATIONAL JOURNAL OF SOLIDS and STRUCTURES

www.elsevier.com/locate/ijsolstr

Influence of imperfect interfaces on bending and vibration of laminated composite shells

Zhen-Qiang Cheng[a,*], Ling-Hui He[a], S. Kitipornchai[b]

[a]*Department of Modern Mechanics, University of Science and Technology of China, Hefei, Anhui 230026, People's Republic of China*
[b]*Department of Civil Engineering, The University of Queensland, Brisbane, Qld. 4072, Australia*

Received 31 July 1997; in revised form 18 September 1998

Abstract

This paper is devoted to modeling elastic behavior of laminated composite shells, with special emphasis on incorporating interfacial imperfection. The conditions of imposing traction continuity and displacement jump across each interface are used to model imperfect interfaces. Vanishing transverse shear stresses on two free surfaces of a shell eliminate the need for shear correction factors. A linear theory underlying elastostatics and kinetics of laminated composite shells in a general configuration is presented from Hamilton's principle. In the special case of vanishing interfacial parameters, this theory reduces to the conventional third-order zigzag theory for perfectly bonded laminated shells. Numerical results for bending and vibration problems of laminated circular cylindrical panels are tabulated and plotted to indicate the influence of the interfacial imperfection.

Nomenclature

θ^i	curvilinear coordinates
t	time
h	shell thickness
${}^{(m)}h$	distance between mth interface and reference surface
μ_α^β	shifter
b_α^β	mixed curvature tensor
a^{ij}	metrics of contravariant bases of reference surface
δ_α^β	mixed Kronecker delta
$v_j,\ V_j$	surface and space components of displacements
e_{ij}	strain tensor

* Corresponding author: Department of Engineering Science and Mechanics, Virginia Polytechnic Institute and State University, Blacksburg, VA 24061-0219, U.S.A.

0020-7683/00/$ - see front matter
PII: S0020-7683(98)00294-7

σ^{ij}	stress tensor
E^{ijkl}	elasticity tensor
${}^{(m)}\Delta V_{\alpha}$	displacement jumps across mth interface
${}^{(m)}R_{\alpha\beta}$	space compliance coefficient of mth interface
u_i, φ_{α}	generalized displacements on reference surface
ρ	mass density
$N^{(J)\alpha}$, $N^{(1)3}$, $M^{(J)\alpha\beta}$	generalized forces and moments
$I^{(J)\alpha\beta}$, $I^{(1)33}$	generalized inertias
L, Φ, r_0	length, central angle and inner radius of cylindrical panel
${}^{(0)}P^3$	external load
$V_{\langle i\rangle}$	physical components of displacement
$\sigma_{\langle ij\rangle}$	physical components of stress
${}^{(m)}R_{\langle\alpha\beta\rangle}$	physical components of compliance coefficient of mth interface.

1. Introduction

The anisotropic constitution of laminated composite structures often results in unique phenomena that can occur at vastly different geometric scales. To investigate random and deterministic heterogeneous particulate and fibrous composites at reinforcement-matrix level, micromechanics-based research is needed. The statistically equivalent single-layer theories for plates and shells are generally capable of accurately describing the global response, whereas at the ply level discrete-layer and zigzag theories are needed to determine the three-dimensional stress field. A comprehensive review can be found in the detailed coverage presented by Reddy (1997) for the first time of traditional theories and refined theories of laminated composite materials. Under the assumption that each lamina is statistically homogeneous and its elastic properties have been determined either by experiments or from micromechanics predictions, this paper only concerns itself with the area at the ply level of laminates.

In most analytical and numerical work on composite materials, a perfect interface between adjacent laminae is assumed which implies continuous displacements and tractions across it. Therefore the interface properties and structures are eliminated, despite the fact that the behavior of composite materials is significantly influenced by the properties of interfaces. In many cases of interest, however, the assumption of a perfect interface is inadequate. Examples for laminated composites could be either the presence of interfacial damage caused by fatigue and environmental effects, or interphase material which may be due to chemical interaction between the constituents or deliberately introduced in order to improve the properties of composites. One of the practical applications has been pointed out by Cheng et al. (1996a) in a class of new composite materials, such as carbon fiber-reinforced aluminum alloy laminates. The idea of weakened interfaces could also be used in smart structures to model an adhesive layer that bonds the actuator to the structural components (Crawley and de Luis, 1987; Reddy and Robbins, 1994). This is because the interphase layer is very thin such that its accurate analysis is unnecessary and almost impossible. In addition, other possible applications can be in layered plates that experience interlayer slip at a precracked interface such as a construction joint of reinforced concrete slabs or the interface of nailed wooden plates (Toledano and Murakami, 1988).

The simplest approach used to characterize the imperfect interface is a linear spring-layer model. The imperfect interface is replaced by a mathematical surface of vanishing thickness across which material properties change discontinuously, with the continuous interfacial tractions being linearly proportional to the displacement jump. Such a model has been efficiently employed in micromechanics-based research at the reinforcement-matrix level (e.g. Aboudi, 1987; Achenbach and Zhu, 1989; Benveniste and Dvorak, 1990; Hashin, 1990, 1991; Qu, 1993a, b; Zhong and Meguid, 1996) and was introduced by Cheng et al.

(1996a, b, 1997) in modeling laminated composite plates with weakened interfaces at the ply level. As an extreme result of vanishing displacement jump, perfect bonding becomes only a special case and thus the theories proposed by Cheng et al. (1996a, b, 1997) can also serve for analyzing mechanical behavior of perfectly bonded laminated plates. In a similar approach, Schmidt and Librescu (1996) have also presented a theoretical formulation for laminated composite plates featuring interlayer slips. As concluded for shells with perfect interfaces (Librescu and Schmidt, 1991; Schmidt and Librescu, 1994), some interesting theorems analogous to three-dimensional elasticity have been noted.

The present work proposes a displacement model satisfying the compatibility conditions for transverse shear stresses both at layer interfaces and on the two free surfaces of the laminated composite shells. As a result, there is no need for the use of shear correction factors and the number of unknowns is shown to be five, irrespective of the number of lamina, i.e. the same number as for the first-order and third-order smeared theories. Hamilton's principle is used to derive the field equations and boundary conditions which underlie linear dynamic response of laminated composite shells in general configuration. Numerical results are given to illustrate the effects of interfacial imperfection on bending and vibration behavior of laminated composite panels.

2. Field equations and boundary conditions

Figure 1 shows an undeformed laminated composite shell consisting of k homogeneous anisotropic laminae with uniform thickness. For convenience, the undeformed lower surface of the shell is chosen as the reference surface defined by $\theta^3 = 0$ and θ^3-axis is normal to the shell surface, where $\{\theta^i\}$ $(i = 1, 2, 3)$ is a curvilinear coordinate system. Let ${}^{(m)}\Omega$ $(m = 0, \ldots, k)$ denote the lower surface $(m = 0)$, the $k-1$ interfaces between the mth and $(m+1)$th laminae $(m = 1, \ldots, k-1)$ and the upper surface $(m = k)$ of the shell. Thus, the mth lamina is among the range of $[{}^{(m-1)}h, {}^{(m)}h]$ in the θ^3-direction, where ${}^{(m)}h$ $(m = 0, \ldots, k)$ is the distance between ${}^{(m)}\Omega$ and ${}^{(0)}\Omega$. Particularly, ${}^{(0)}h = 0$ and ${}^{(k)}h = h$, where h denotes the total thickness of the shell.

In the following developments, $(\ )_{,i}$ denotes a partial derivative with respect to the corresponding

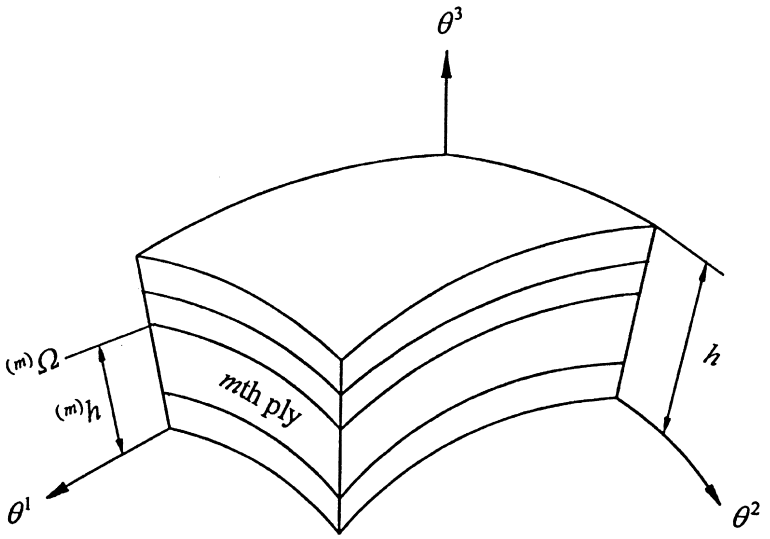

Fig. 1. Geometry of a laminated shell.

spatial coordinate, while $(\ )_{\|i}$ and $(\ )_{|\alpha}$ designate covariant derivatives with respect to the space and the reference surface metrics, respectively. The Einsteinian summation convention applies to repeated indices of tensor components where Latin indices ranging from 1 to 3 while Greek indices are from 1 to 2. The partial derivative of the Heaviside step function $\mathrm{H}(\theta^3 - {}^{(m)}h)$ with respect to θ^3 is stipulated as the right-hand one, thus $\mathrm{H}_{,3}(\theta^3 - {}^{(m)}h) = 0$.

The general representation of displacements for any point of the shell can be written, with respect to the contravariant bases of the reference surface, as

$$v_j(\theta^i; t) = \sum_{m=0}^{k-1}\sum_{n=0}^{\infty} {}^{(m)}u_j^{(n)}(\theta^\alpha; t)(\theta^3 - {}^{(m)}h)^n \mathrm{H}(\theta^3 - {}^{(m)}h), \tag{1}$$

where the term ${}^{(m)}u_j^{(0)}(\theta^\alpha; t)$, which was excluded for perfect interfaces by He (1994, 1995), has been retained in the present theory. This term represents a displacement jump across the interface ${}^{(m)}\Omega$ and hence provides a possible incorporation of imperfect interfaces of laminated shells, e.g. weakened bonding or even delamination. The case of a perfect interface corresponds to this term being zero.

The displacements of the space components can be expressed in terms of their shifted surface components as

$$V_\alpha = \mu_\alpha^\beta v_\beta, \quad V_3 = v_3, \tag{2}$$

and the covariant derivatives of the space components are connected with their surface counterparts as (Naghdi, 1963; Librescu, 1975)

$$V_{\alpha\|\beta} = \mu_\alpha^\nu\left(v_{\nu|\beta} - b_{\nu\beta}v_3\right), \quad V_{\alpha\|3} = \mu_\alpha^\nu v_{\nu,3}, \quad V_{3\|\alpha} = v_{3,\alpha} + b_\alpha^\nu v_\nu, \quad V_{3\|3} = v_{3,3}, \tag{3}$$

with

$$\mu_\alpha^\beta = \delta_\alpha^\beta - \theta^3 b_\alpha^\beta, \quad b_\alpha^\beta = -\Gamma_{\alpha 3}^\beta|_{({}^{(0)}\Omega)}, \quad b_{\alpha\beta} = \Gamma_{\alpha\beta}^3|_{({}^{(0)}\Omega)}, \tag{4}$$

where δ_α^β is the mixed Kronecker delta function, $\Gamma_{jk}^i|_{({}^{(0)}\Omega)}$ denotes the Christoffel symbol of the second kind with respect to ${}^{(0)}\Omega$.

The strain component e_{ij} and stress component σ^{ij} of the shell are expressed as

$$e_{ij} = \frac{1}{2}\left(V_{i\|j} + V_{j\|i}\right), \quad \sigma^{\alpha\beta} = H^{\alpha\beta\omega\rho}e_{\omega\rho}, \quad \sigma^{\alpha 3} = 2E^{\alpha 3\omega 3}e_{\omega 3}, \tag{5}$$

where E^{ijkl} is the space component of the elastic moduli associated with an elastic anisotropic body, and $H^{\alpha\beta\omega\rho} = E^{\alpha\beta\omega\rho} - E^{\alpha\beta 33}E^{33\omega\rho}/E^{3333}$. The second and third parts of eqn (5) hold valid only under the assumptions that each lamina possesses elastic symmetry with respect to surfaces parallel to ${}^{(0)}\Omega$ and that σ^{33} is vanishingly small.

As used for the case of laminated plates, the spring-layer model characterizing an imperfect interface in shear is

$$\sigma^{\beta 3}(\theta^\rho, {}^{(m)}h^+; t) = \sigma^{\beta 3}(\theta^\rho, {}^{(m)}h^-; t), \quad {}^{(m)}\Delta V_\alpha = {}^{(m)}R_{\alpha\beta}(\theta^\rho)\sigma^{\beta 3}(\theta^\rho, {}^{(m)}h; t), \quad (m = 1, \ldots, k-1), \tag{6}$$

where ${}^{(m)}R_{\alpha\beta}$ represents the space compliance coefficient of the mth spring-layer interface ${}^{(m)}\Omega$. A detailed discussion on this model may be found in the work of Cheng et al. (1996a, b, 1997). It is emphasized that the interface parameter ${}^{(m)}R_{\alpha\beta}$ depending upon θ^ρ implies the non-uniform bonding strength at the interface ${}^{(m)}\Omega$ $(m = 1, \ldots, k-1)$, i.e., the most general form of interfacial imperfection in shear is incorporated in the present theory. The vanishing ${}^{(m)}R_{\alpha\beta}$ corresponds to the mth interface being

perfect. A slightly weakened interface may be modeled by small values of ${}^{(m)}R_{\alpha\beta}$, which are spatial functions. This means that different interfacial bonding strength on the interfacial area can be characterized by different values of the interfacial parameter.

Based on a three-phase model and generalized self-consistent scheme for random composites, a theoretical evaluation of interfacial parameters was made by Hashin (1991) in terms of interphase characteristics for isotropic deformation. However, such an efficient scheme only applies to random composites. Further theoretical work is needed on the estimation of the interfacial parameters, which requires a knowledge of interfacial microstructures and is beyond the scope of this paper. In an alternative way they can be determined experimentally either by direct shear test or through statistically equivalent macroscopic moduli for imperfectly bonded layered media (Lai et al., 1997), in turn to determine the interfacial damage parameters.

From the foregoing, an approximate displacement model for laminated composite shells may be proposed as

$$v_\alpha(\theta^i;t)=\mu_\alpha^\beta u_\beta-\theta^3u_{3,\alpha}+h_\alpha^\beta\varphi_\beta,\ v_3(\theta^i;t)=u_3, \tag{7}$$

where u_i and φ_α are independent of the coordinate θ^3, an overview of the development for obtaining the expression of h_α^β can be found in Appendix A. This model has ensured the fulfillment of vanishing transverse shear stresses on the two free surfaces and continuous tractions across interfaces.

It is assumed that the mass density ρ is independent of time t and that arbitrarily distributed normal loads ${}^{(0)}p^3(\theta^\alpha;t)$ and ${}^{(k)}p^3(\theta^\alpha;t)$ are applied to the lower surface ${}^{(0)}\Omega$ and the upper surface ${}^{(k)}\Omega$, respectively. From Hamilton's principle

$$\int_0^{t_0}\left(\int_V\sigma^{ij}\delta e_{ij}\,\mathrm{d}V-\int_V\dot{V}^i\delta\dot{V}_i\rho\,\mathrm{d}V-\int_\Omega p^3\delta V_3\,\mathrm{d}\Omega\right)\mathrm{d}t=0, \tag{8}$$

the dynamic field equations are derived as

$$\begin{aligned}
&M^{(1)\alpha\beta}_{|\beta}-N^{(1)\alpha}-I^{(1)\beta\alpha}\ddot{u}_\beta+I^{(2)\beta\alpha}\ddot{u}_{3,\beta}-I^{(3)\beta\alpha}\ddot{\varphi}_\beta=0,\\
&M^{(2)\alpha\beta}_{|\alpha\beta}+N^{(1)3}+P^3-I^{(1)33}\ddot{u}_3-\left(I^{(2)\beta\alpha}\ddot{u}_\alpha\right)_{|\beta}+\left(I^{(4)\alpha\beta}\ddot{u}_{3,\alpha}\right)_{|\beta}-\left(I^{(6)\alpha\beta}\ddot{\varphi}_\alpha\right)_{|\beta}=0,\\
&M^{(3)\alpha\beta}_{|\beta}-N^{(2)\alpha}-N^{(3)\alpha}-I^{(3)\alpha\beta}\ddot{u}_\beta+I^{(6)\alpha\beta}\ddot{u}_{3,\beta}-I^{(5)\beta\alpha}\ddot{\varphi}_\beta=0,
\end{aligned} \tag{9}$$

associated with either one of each of the following pairs of boundary conditions

$$\begin{aligned}
&n_\beta M^{(1)\alpha\beta}=0,\quad\text{or}\ \delta u_\alpha=0,\\
&n_\beta\left(M^{(2)\beta\alpha}_{|\alpha}-I^{(2)\beta\alpha}\ddot{u}_\alpha+I^{(4)\alpha\beta}\ddot{u}_{3,\alpha}-I^{(6)\alpha\beta}\ddot{\varphi}_\alpha\right)=0,\quad\text{or}\ \delta u_3=0,\\
&n_\beta M^{(3)\alpha\beta}=0,\quad\text{or}\ \delta\varphi_\alpha=0,\\
&n_\beta M^{(2)\alpha\beta}=0,\quad\text{or}\ \delta u_{3,\alpha}=0,
\end{aligned} \tag{10}$$

where

$$\left[N^{(1)\alpha}, N^{(2)\alpha}, N^{(1)3}\right] = \int_0^h \sigma^{\lambda\beta}\mu_\lambda^\nu\left[\mu_{\nu|\beta}^\alpha, h_{\nu|\beta}^\alpha, b_{\nu\beta}\right]\mu\,\mathrm{d}\theta^3, \tag{11}$$

$$N^{(3)\alpha} = \int_0^h \sigma^{\lambda 3}\left(\mu_\lambda^\nu h_{\nu,3}^\alpha + b_\lambda^\nu h_\nu^\alpha\right)\mu\,\mathrm{d}\theta^3, \tag{12}$$

$$\left[M^{(1)\alpha\beta}, M^{(2)\alpha\beta}, M^{(3)\alpha\beta}\right] = \int_0^h \sigma^{\lambda\beta}\mu_\lambda^\nu\left[\mu_\nu^\alpha, \theta^3\delta_\nu^\alpha, h_\nu^\alpha\right]\mu\,\mathrm{d}\theta^3, \tag{13}$$

$$\begin{aligned}\left[I^{(1)\alpha\beta}, I^{(2)\alpha\beta}, I^{(3)\alpha\beta}, I^{(4)\alpha\beta}, I^{(5)\alpha\beta}, I^{(6)\alpha\beta}\right] = \int_0^h \rho a^{\lambda\nu}\Big[&\mu_\nu^\alpha\mu_\lambda^\beta, \theta^3\delta_\nu^\alpha\mu_\lambda^\beta, h_\nu^\alpha\mu_\lambda^\beta, \left(\theta^3\right)^2\delta_\nu^\alpha\delta_\lambda^\beta, h_\nu^\alpha h_\lambda^\beta,\\ &\theta^3 h_\nu^\alpha\delta_\lambda^\beta\Big]\mu\,\mathrm{d}\theta^3,\end{aligned} \tag{14}$$

$$I^{(1)33} = \int_0^h \rho\mu\,\mathrm{d}\theta^3, \tag{15}$$

$$P^3 = {}^{(k)}\mu^{(k)}p^3 + {}^{(0)}p^3, \tag{16}$$

$a^{\alpha\beta}$ in eqn (14) is the metrics of contravariant bases referred to the reference surface, and

$$\mu = \det\left(\mu_\alpha^\beta\right), \quad {}^{(k)}\mu = \mu|_{{}^{(k)}\Omega}. \tag{17}$$

For brevity, displacement-based field equations are given in Appendix B. These equations need to be solved with the boundary conditions of eqn (10) to obtain the unknowns u_i and φ_α for any set of shell parameters and the load parameter P^3. The case of quasi-static deformation of the laminated shell featuring interfacial damage coincides with the linear counterpart of Cheng and Kitipornchai (1998). The field equations and boundary conditions given by Cheng et al. (1996a) are recovered from the present work in the special case of flat laminated plates. By setting ${}^{(m)}R_{\alpha\beta} = 0$ $(m = 1, \ldots, k-1)$, the present field equations and boundary conditions become those for perfect bonding. They are exactly the same as those given by He (1994), and are also very similar to those proposed by Di Sciuva and Icardi (1993) and Xavier et al. (1993, 1995).

3. Numerical example

The present theory can be applied to solve a wide range of complicated problems. However, complete solutions to such problems require the determination of interface parameters either through theoretical evaluation of interfacial properties and microstructures or experimental measurements. Since the evaluation of such parameters is beyond the scope of this paper, the influence of interfacial imperfection on the global and local behavior of laminated composite shells will be investigated by restricting attention to the effects of imperfect interfaces on their linear bending and vibration behavior. An orthotropic laminated circular cylindrical panel of length L, central angle Φ and inner radius r_0 will be used as the example for analyzing such interfacial imperfection. The panel is simply supported at edges $\theta^1 = 0, L$ and $\theta^2 = 0, \Phi$. Identically uniform bonding of the interfaces is assumed.

Under the action of transverse normal pressure

$$^{(0)}P^3 = p_0 \sin\left(\frac{m_1\pi\theta^1}{L}\right)\sin\left(\frac{m_2\pi\theta^2}{\Phi}\right)e^{i\omega t} \tag{18}$$

on the inner surface of the panel, exact solutions can easily be given for static bending ($m_1 = m_2 = 1, \omega = 0$), and for free flexural vibration ($p_0 = 0$). Details for obtaining closed-form solutions are given in Appendix C for brevity.

For the geometry of the circular cylindrical panel, the following quantities are useful

$$a^{11} = 1, \quad a^{22} = \frac{1}{r_0^2}, \quad a^{12} = a^{21} = 0,$$

$$b_{11} = 0, \quad b_{22} = -r_0, \quad b_{12} = b_{21} = 0,$$

$$\mu_1^1 = 1, \quad \mu_2^2 = 1 + \frac{\theta^3}{r_0}, \quad \mu_1^2 = \mu_2^1 = 0. \tag{19}$$

The physical components of tensors in the orthogonal bases are then defined by

$$^{(m)}R_{\langle 11\rangle} = {}^{(m)}R_{11}, \quad {}^{(m)}R_{\langle 12\rangle} = \frac{1}{r_0+\theta^3}{}^{(m)}R_{12}, \quad {}^{(m)}R_{\langle 22\rangle} = \frac{1}{\left(r_0+\theta^3\right)^2}{}^{(m)}R_{22},$$

$$V_{\langle 1\rangle} = v_1, \quad V_{\langle 3\rangle} = v_3, \quad V_{\langle 2\rangle} = \frac{1}{r_0}v_2, \quad \sigma_{\langle 11\rangle} = \sigma^{11}, \quad \sigma_{\langle 13\rangle} = \sigma^{13},$$

$$\sigma_{\langle 12\rangle} = \left(r_0+\theta^3\right)\sigma^{12}, \quad \sigma_{\langle 23\rangle} = \left(r_0+\theta^3\right)\sigma^{23}, \quad \sigma_{\langle 22\rangle} = \left(r_0+\theta^3\right)^2\sigma^{22}. \tag{20}$$

See Naghdi (1963) for more details. After the transformation (20), the quantities with subscripts enclosed by a pair of angle brackets become physically meaningful, e.g. the physical meaning of $^{(m)}R_{\langle\alpha\beta\rangle}$ is the compliance coefficient of the mth spring-layer interface.

With these physical components, the following dimensionless quantities are introduced as

$$S = \frac{r_0}{h} + 0.5, \quad \bar{V}_{\langle\alpha\rangle} = \frac{10E_L}{p_0hS^3}V_{\langle\alpha\rangle}, \quad \bar{V}_{\langle 3\rangle} = \frac{10E_L}{p_0hS^4}V_{\langle 3\rangle},$$

$$\bar{\sigma}_{\langle\alpha\beta\rangle} = \frac{10}{p_0S^2}\sigma_{\langle\alpha\beta\rangle}, \quad \bar{\sigma}_{\langle\alpha 3\rangle} = \frac{10}{p_0S}\sigma_{\langle\alpha 3\rangle}, \quad \bar{\omega} = \left(\frac{L}{h}\right)^2\sqrt{\frac{\rho h^2}{E_LS}}\omega. \tag{21}$$

The material chosen for numerical computation is a laminated panel composed of unidirectionally aligned fibrous composites, with identical density, thickness and stiffness properties for each lamina, unless otherwise indicated,

$$E_L/E_T = 25, \quad G_{LT}/E_T = 0.5, \quad G_{TT}/E_T = 0.2, \quad v_{LT} = v_{TT} = 0.25, \tag{22}$$

where E is the tensile modulus, G is the shear modulus, v is Poisson's ratio and the subscripts L and T refer to the directions parallel and normal to the fibers, respectively.

Table 1
Central deflection and stresses of a three-ply (90°/0°/90°) laminated circular cylindrical panel under sinusoidal loading

S		VB (1991)	$\bar{R}=0$	$\bar{R}=0.3$	$\bar{R}=0.6$	$\bar{R}=0.9$
4	$\bar{V}_{\langle 3\rangle}\left(\frac{L}{2},\frac{\Phi}{2},0\right)$	4.00	3.60671	4.54355	5.22412	5.68617
10		1.223	1.20335	1.56068	1.95346	2.36049
50		0.5495	0.54862	0.56474	0.58443	0.60760
100		0.4715	0.47110	0.47432	0.47827	0.48293
500		0.1027	0.10269	0.10270	0.10271	0.10272
4	$\bar{\sigma}_{\langle 11\rangle}\left(\frac{L}{2},\frac{\Phi}{2},0\right)$	−0.2701	−0.12923	−0.15659	−0.17584	−0.18821
10		−0.0791	−0.05632	−0.06436	−0.07327	−0.08248
50		−0.0225	−0.02167	−0.02139	−0.02106	−0.02067
100		0.0018	0.00197	0.00220	0.00247	0.00280
500		0.0379	0.03788	0.03788	0.03789	0.03789
4	$\bar{\sigma}_{\langle 11\rangle}\left(\frac{L}{2},\frac{\Phi}{2},h\right)$	0.1270	0.12126	0.14641	0.16369	0.17444
10		0.0739	0.07231	0.08561	0.10028	0.11544
50		0.0712	0.07097	0.07215	0.07360	0.07531
100		0.0838	0.08370	0.08406	0.08450	0.08502
500		0.0559	0.05585	0.05585	0.05586	0.05586
4	$\bar{\sigma}_{\langle 22\rangle}\left(\frac{L}{2},\frac{\Phi}{2},0\right)$	−9.323	−10.52806	−12.94523	−14.80410	−16.14023
10		−5.224	−5.30760	−6.04312	−6.87232	−7.74757
50		−3.987	−3.98701	−4.01326	−4.04618	−4.08560
100		−3.507	−3.50626	−3.50900	−3.51255	−3.51690
500		−0.7542	−0.75451	−0.75437	−0.75419	−0.75399
4	$\bar{\sigma}_{\langle 22\rangle}\left(\frac{L}{2},\frac{\Phi}{2},h\right)$	6.545	7.01022	8.51118	9.67634	10.52132
10		4.683	4.69967	5.30698	5.99277	6.71749
50		3.930	3.92646	3.95217	3.98441	4.02301
100		3.507	3.50478	3.50766	3.51137	3.51592
500		0.7895	0.78973	0.78959	0.78941	0.78921
4	$\sigma_{\langle 12\rangle}(0,0,0)$	0.1609	0.16242	0.19470	0.21369	0.22264
10		0.0729	0.07569	0.09431	0.11447	0.13494
50		0.0760	0.07639	0.07826	0.08055	0.08324
100		0.1038	0.10393	0.10455	0.10532	0.10622
500		0.0889	0.08886	0.08886	0.08887	0.08887
4	$\sigma_{\langle 12\rangle}(0,0,h)$	−0.1081	−0.08998	−0.01483	−0.11201	−0.11367
10		−0.0374	−0.03343	−0.03944	−0.04575	−0.05193
50		0.0118	0.01228	0.01302	0.01391	0.01496
100		0.0478	0.04798	0.04840	0.04891	0.04951
500		0.0766	0.07660	0.07660	0.07661	0.07662
4	$\bar{\sigma}_{\langle 13\rangle}\left(0,\frac{\Phi}{2},\frac{h}{3}\right)$	0.1736	0.13683	0.15432	0.16014	0.15798
10		0.0826	0.07746	0.09270	0.10888	0.12495
50		0.0894	0.08904	0.09096	0.09329	0.09604
100		0.1223	0.12213	0.12280	0.12363	0.12460
500		0.1051	0.10509	0.10509	0.10510	0.10511
4	$\bar{\sigma}_{\langle 23\rangle}\left(\frac{L}{2},0,\frac{h}{2}\right)$	2.329	2.00375	1.49511	1.09511	0.80258
10		3.264	3.24028	3.06610	2.86781	2.65714
50		3.491	3.48937	3.47683	3.46121	3.44259
100		3.127	3.12561	3.12009	3.11325	3.10511
500		0.691	0.69088	0.69068	0.69044	0.69015

$L/h=4S, \Phi=\pi/4$.

Table 2
Central deflection and stresses of a two-ply (0°/90°) laminated circular cylindrical panel under sinusoidal loading

S		VB (1991)	$\bar{R}=0$	$\bar{R}=0.3$	$\bar{R}=0.6$	$\bar{R}=0.9$
4	$\bar{V}_{\langle 3\rangle}\left(\frac{L}{2},\frac{\Phi}{2},0\right)$	6.100	5.09696	5.37359	5.58604	5.73422
10		3.330	3.16576	3.23447	3.30525	3.37701
50		2.242	2.23717	2.23920	2.24141	2.24378
100		1.367	1.36665	1.36686	1.36710	1.36736
500		0.1005	0.10049	0.10049	0.10049	0.10049
4	$\bar{\sigma}_{\langle 11\rangle}\left(\frac{L}{2},\frac{\Phi}{2},0\right)$	−0.9600	−0.71888	−0.75165	−0.77769	−0.79659
10		−0.1689	−0.15665	−0.15947	−0.16267	−0.16619
50		1.610	1.60510	1.60612	1.60720	1.60834
100		2.300	2.29788	2.29808	2.29830	2.29853
500		0.9436	0.94359	0.94359	0.94359	0.94359
4	$\bar{\sigma}_{\langle 11\rangle}\left(\frac{L}{2},\frac{\Phi}{2},h\right)$	0.2120	0.20710	0.21350	0.21842	0.22183
10		0.1930	0.19098	0.19327	0.19566	0.19811
50		0.2189	0.21866	0.21883	0.21901	0.21921
100		0.1871	0.18708	0.18711	0.18715	0.18719
500		0.0449	0.04491	0.04491	0.04491	0.04491
4	$\bar{\sigma}_{\langle 22\rangle}\left(\frac{L}{2},\frac{\Phi}{2},0\right)$	−1.789	−1.11616	−1.02562	0.94065	−0.86547
10		−1.343	−1.20498	−1.18396	−1.16099	−1.13648
50		−0.9670	−0.96152	−0.96055	−0.95946	−0.95826
100		−0.5759	−0.57495	−0.57475	−0.57453	−0.57428
500		−0.0339	−0.03392	−0.03392	−0.03392	−0.03391
4	$\bar{\sigma}_{\langle 22\rangle}\left(\frac{L}{2},\frac{\Phi}{2},h\right)$	10.31	12.07122	12.70830	13.27148	13.74040
10		10.59	10.95205	11.10224	11.26302	11.43170
50		8.937	8.95433	8.95822	8.96262	8.96753
100		5.560	5.56430	5.56450	5.56475	5.56506
500		0.4345	0.43460	0.43460	0.43460	0.43460
4	$\bar{\sigma}_{\langle 12\rangle}(0,0,0)$	0.2812	0.22653	0.22952	0.23104	0.23128
10		0.2325	0.22105	0.22265	0.22425	0.22581
50		0.3449	0.34440	0.34463	0.34487	0.34514
100		0.3452	0.34514	0.34519	0.34524	0.34530
500		0.1045	0.10448	0.10448	0.10449	0.10449
4	$\bar{\sigma}_{\langle 12\rangle}(0,0,h)$	−0.2007	−0.16858	−0.16711	−0.16463	−0.16148
10		−0.1247	−0.11819	−0.11803	−0.11781	−0.11752
50		0.0784	0.07842	0.07849	0.07855	0.07862
100		0.1819	0.18187	0.18188	0.18188	0.18188
500		0.0925	0.09245	0.09245	0.09245	0.09245
4	$\bar{\sigma}_{\langle 13\rangle}\left(0,\frac{\Phi}{2},\frac{h}{4}\right)$	0.2758	0.21269	0.21215	0.21053	0.20812
10		0.1591	0.15053	0.15054	0.15051	0.15044
50		−0.0448	−0.04424	−0.04428	−0.04432	−0.04436
100		−0.1512	−0.15097	−0.15097	−0.15097	−0.15097
500		−0.0841	−0.08409	−0.08409	−0.08409	−0.08409
4	$\bar{\sigma}_{\langle 23\rangle}\left(\frac{L}{2},0,\frac{3h}{4}\right)$	4.440	5.48863	5.73007	5.95882	6.16301
10		5.457	5.68891	5.73936	5.79491	5.85457
50		4.785	4.79505	4.79597	4.79707	4.79837
100		2.972	2.97454	2.97446	2.97440	2.97436
500		0.227	0.22746	0.22746	0.22745	0.22745

$L/h=4S, \Phi=\pi/4$.

The interface parameters are taken as ${}^{(m)}R_{\langle\alpha\beta\rangle} = \delta_{\alpha\beta}\bar{R}h/E_T$ for each lamina, where $\bar{R}$ is a dimensionless quantity and $\delta_{\alpha\beta}$ is the Kronecker delta symbol. This assumption leads to ${}^{(m)}\Delta V_{\langle\alpha\rangle} = \bar{R}h\sigma_{\langle\alpha 3\rangle}/E_T$. It means that the interfaces of the laminated shells are equally weakened. The degree of weakness of each interface is uniform in all directions and locations, and equal degree of weakness is assumed for all interfaces.

Tables 1 and 2 show the dimensionless central deflection and stresses of three-ply and two-ply panels for various values of $\bar{R}$, together with comparative benchmark results given by Varadan and Bhaskar (1991) (denoted as VB, 1991 in Tables 1 and 2, as well as in Figs. 2–8) for perfect interfaces calculated from three-dimensional elasticity. As is well known in the literature, most theories for perfectly bonded plates and shells, which make use of a priori assumption of through-the-thickness displacement distribution, fail to predict sufficiently accurately the transverse shear stresses for moderately thick and very thick plates and shells directly from the constitutive equations, even though interface continuity conditions of tractions and displacements have been imposed. Instead, they are evaluated accurately from the equilibrium equations. In similar fashion, the trend of curves showing variations of the interfacial stresses with $\bar{R}$ calculated directly from constitutive relations seems to be physically unreasonable, see the work by Cheng et al. (1996a). Therefore the transverse shear stresses in Tables 1 and 2, as well as in Figs. 7 and 8, were calculated from the equilibrium equation $\sigma^{\alpha k}_{\|k} = 0$. Some comments on the use of an a posteriori calculation of such components by means of three-dimensional equilibrium and constitutive relations were given by Noor and Peters (1989), Noor and Burton (1990)

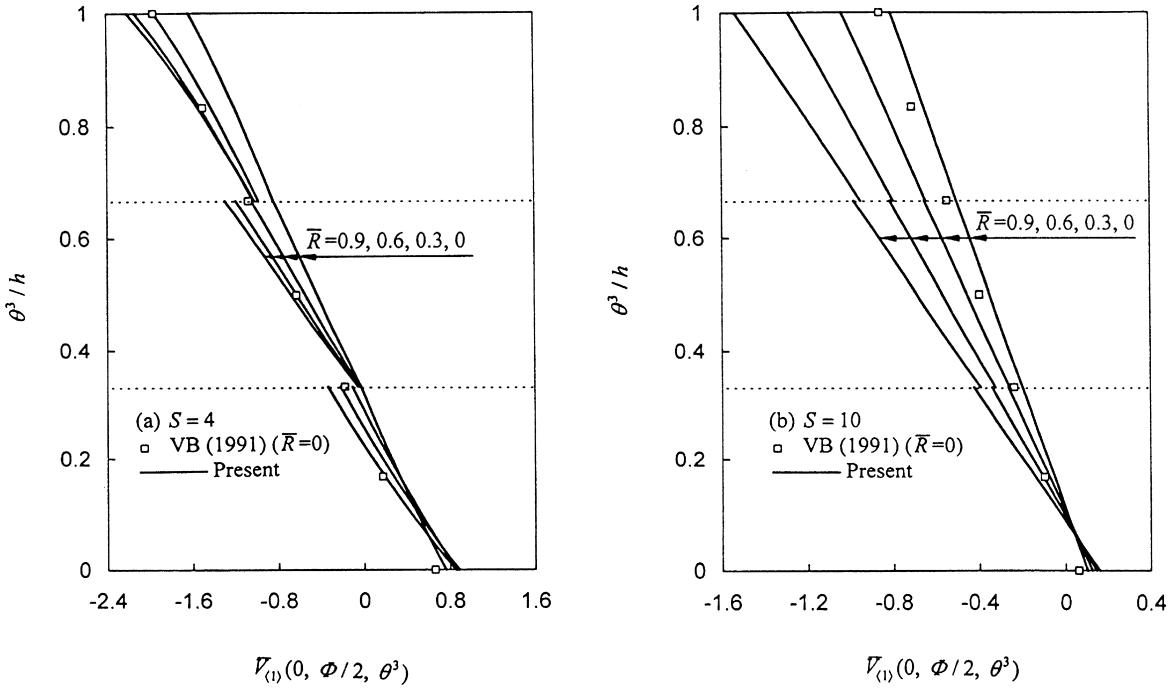

Fig. 2. (a, b) Through-the-thickness in-surface displacement $\bar{V}_{\langle 1\rangle}$ of a three-ply (90°/0°/90°) laminated circular cylindrical panel ($L/h = 4S, \Phi = \pi/4$).

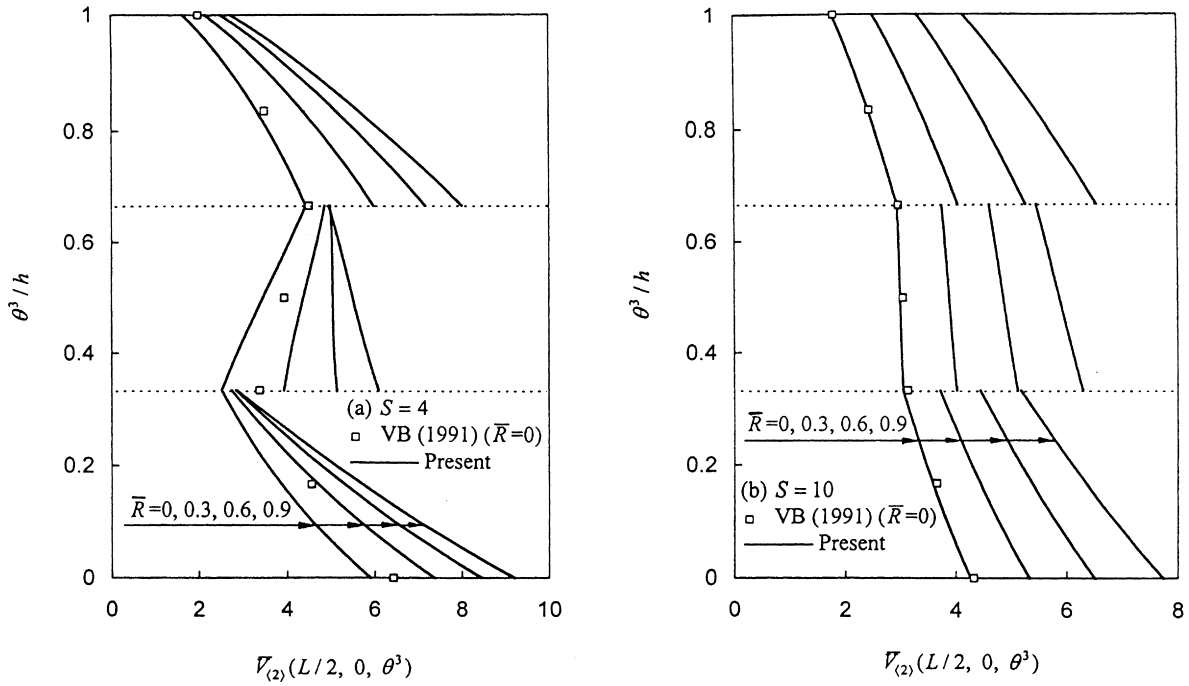

Fig. 3. (a, b) Through-the-thickness in-surface displacement $\bar{V}_{\langle 2\rangle}$ of a three-ply (90°/0°/90°) laminated circular cylindrical panel ($L/h = 4S, \Phi = \pi/4$).

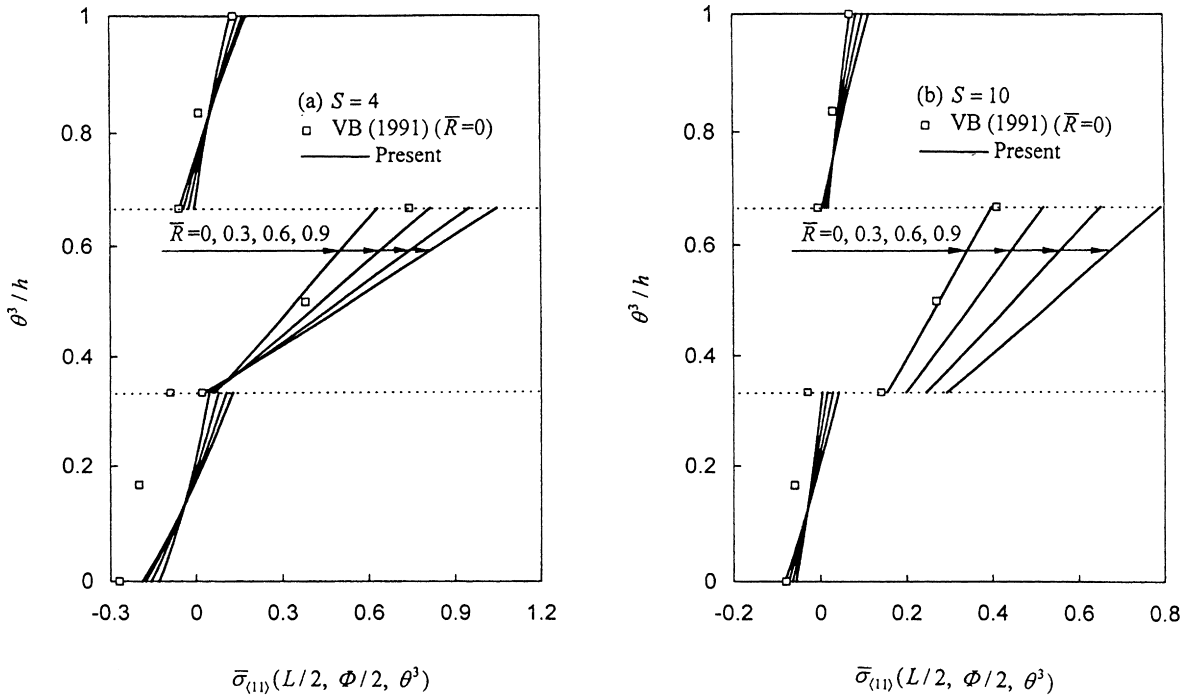

Fig. 4. (a, b) Through-the-thickness bending stress $\bar{\sigma}_{\langle 11\rangle}$ of a three-ply (90°/0°/90°) laminated circular cylindrical panel ($L/h = 4S, \Phi = \pi/4$).

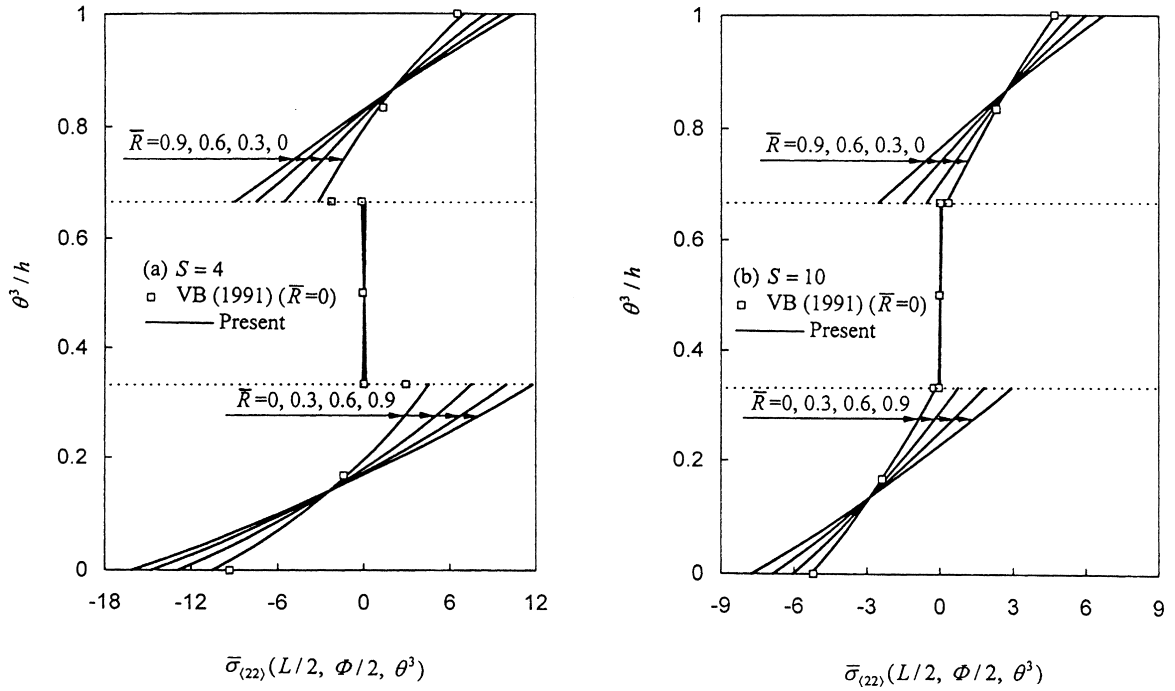

Fig. 5. (a, b) Through-the-thickness bending stress $\bar{\sigma}_{\langle 22\rangle}$ of a three-ply (90°/0°/90°) laminated circular cylindrical panel ($L/h = 4S, \Phi = \pi/4$).

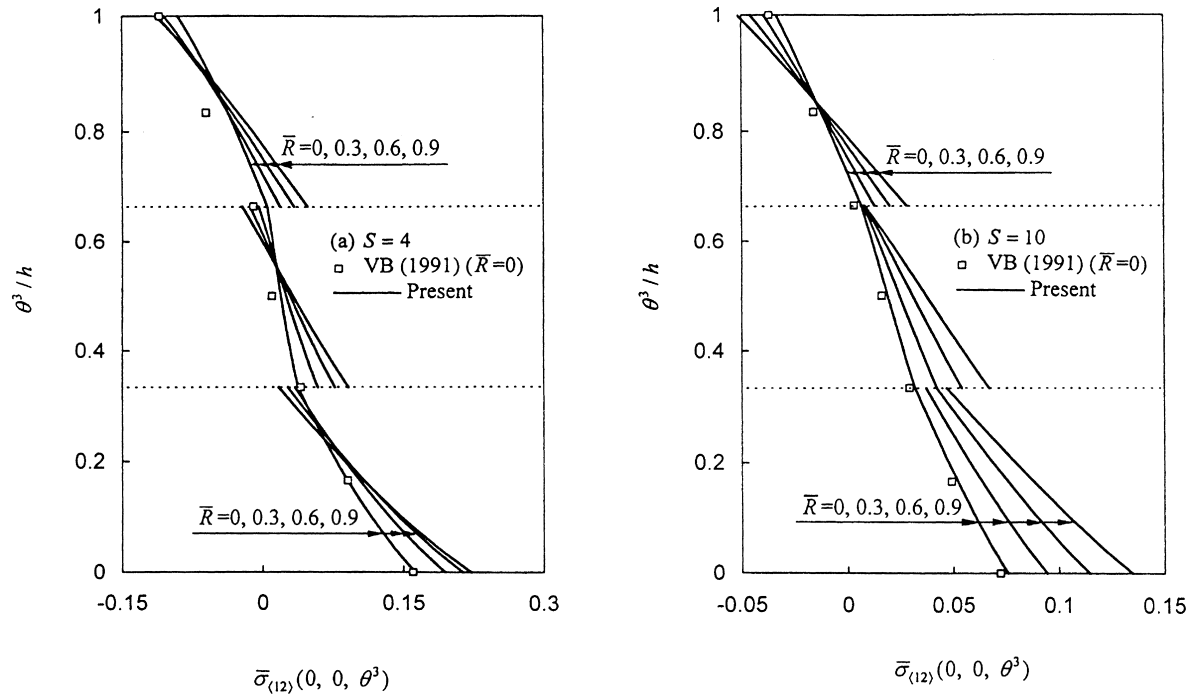

Fig. 6. (a, b) Through-the-thickness bending stress $\bar{\sigma}_{\langle 12\rangle}$ of a three-ply (90°/0°/90°) laminated circular cylindrical panel ($L/h = 4S, \Phi = \pi/4$).

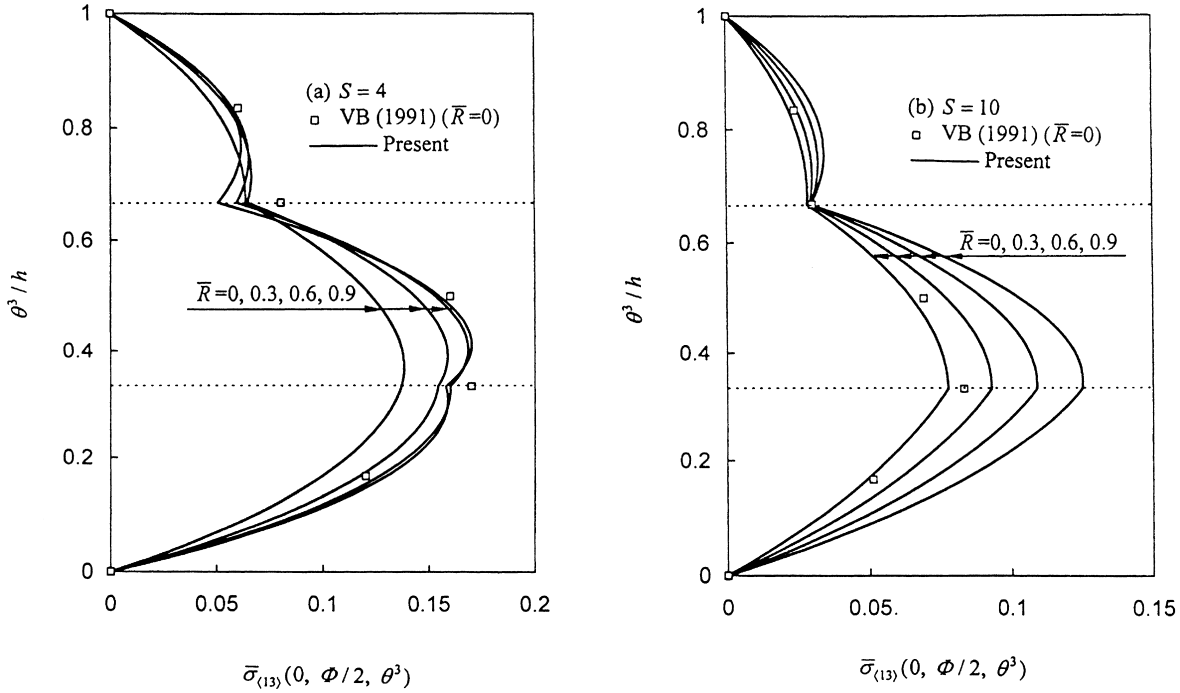

Fig. 7. (a, b) Through-the-thickness transverse shear stress $\bar{\sigma}_{\langle 13\rangle}$ of a three-ply (90°/0°/90°) laminated circular cylindrical panel ($L/h = 4S, \Phi = \pi/4$).

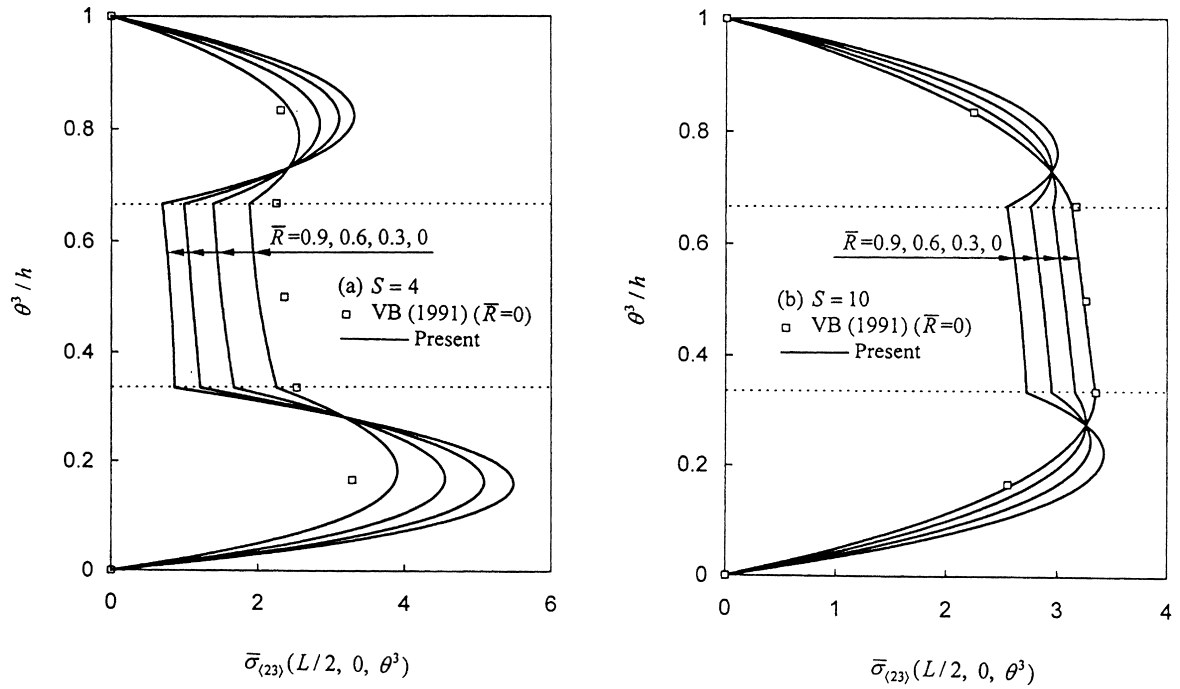

Fig. 8. (a, b) Through-the-thickness transverse shear stress $\bar{\sigma}_{\langle 23\rangle}$ of a three-ply (90°/0°/90°) laminated circular cylindrical panel ($L/h = 4S, \Phi = \pi/4$).

Table 3
Natural frequencies of a three-ply (90°/0°/90°) laminated circular cylindrical panel

S	(m_1, m_2)	XCL(1995)	$\bar{R}=0$	$\bar{R}=0.3$	$\bar{R}=0.6$	$\bar{R}=0.9$
4	(1,1)	12.06	11.99395	10.46062	9.51144	8.90386
10		12.99	12.95592	11.66571	10.57431	9.67627
20		11.25	11.23782	10.76221	10.26312	9.76555
50		8.20	8.20638	8.14615	8.07443	7.99254
100		7.11	7.11737	7.10816	7.09693	7.08374
500		10.68	10.70899	10.70894	10.70888	10.70881
4	(2, 1)	12.45	12.38716	10.89474	9.97441	9.38532
10		13.59	13.56426	12.32296	11.28327	10.43676
20		12.41	12.41403	11.97924	11.52694	11.08049
50		11.47	11.50035	11.45682	11.40519	11.34654
100		13.33	13.37722	13.37225	13.36619	13.35909
500		27.33	27.45223	27.45221	27.45218	27.45216
4	(1, 2)	34.88	34.63088	32.53590	31.71714	31.43851
10		39.85	39.67459	34.31803	30.72844	28.27173
20		41.21	41.30724	37.13336	33.59432	30.67520
50		32.72	32.70070	31.69756	30.59182	29.43239
100		24.19	24.18117	23.97007	23.71829	23.43030
500		11.45	11.44624	11.44239	11.43766	11.43205
4	(2, 2)	34.98	34.73297	32.64673	31.82869	31.54784
10		39.96	39.78115	34.43379	30.85229	28.40182
20		41.53	41.42976	37.25946	33.72556	30.81249
50		32.94	32.91889	31.91951	30.81842	29.66449
100		24.66	24.65934	24.45170	24.20414	23.92110
500		15.42	15.43436	15.43149	15.42797	15.42380

$L/h = 5S, \Phi = \pi/3$.

and Lee and Cao (1996). Tables 3 and 4 give the first four frequencies of three-ply and two-ply composite panels. Tables 5 and 6 show frequency values of three-ply panel for different values of Φ or E_L/E_T when vibrating in its fundamental flexural mode. The higher-order zigzag solution obtained by Xavier et al. (1995) (denoted as XCL, 1995 in Tables 3–6) for perfect interfaces is also given for comparison.

When the theory is used to consider the special case of perfect interfaces, the present results for $\bar{R}=0$ are exactly the same as given by He (1994). In that paper, as well as the paper by Xavier et al. (1993), comparison has been made with an exact three-dimensional elasticity solution and several other shell theories, confirming the high accuracy achieved and the necessity of using the third-order zigzag approach. Therefore, assessment of the present theory for the case of perfect bonding is unnecessary. It is worth noting that there are two causes for slight difference between the present results for perfect interfaces and the results given by Xavier et al. (1993, 1995) for vibration problems as shown in Tables 3–6 and for bending problems which are not given herein. One results from slightly different displacement assumptions, while another is due to the different choices of the reference surface. The location of the reference surface is related with, e.g. for a circular cylindrical shell, the term $h/(r_0+h_0)$, where h_0 denotes the distance between the reference surface and the lower surface of the shell, being zero for the present theory and $h/2$ for the theory of Xavier et al. (1993, 1995). The term h/r_0 is

Table 4
Natural frequencies of a two-ply (90°/0°) laminated circular cylindrical panel

S	(m_1, m_2)	XCL (1995)	$\bar{R}=0$	$\bar{R}=0.3$	$\bar{R}=0.6$	$\bar{R}=0.9$
4	(1, 1)	11.13	10.78996	10.53890	10.32897	10.15966
10		7.87	7.82445	7.77139	7.71659	7.66071
20		5.96	5.95669	5.94678	5.93612	5.92475
50		5.05	5.05347	5.05260	5.05165	5.05060
100		5.71	5.72609	5.72595	5.72579	5.72561
500		11.51	11.54561	11.54560	11.54559	11.54558
4	(2, 1)	11.85	11.53170	11.26504	11.03931	10.85434
10		9.06	9.03172	8.97776	8.92138	8.86327
20		8.15	8.16766	8.15808	8.14752	8.13603
50		9.74	9.77587	9.77479	9.77355	9.77213
100		12.97	13.02946	13.02916	13.02881	13.02840
500		28.32	28.45987	28.45984	28.45981	28.45978
4	(1, 2)	37.89	35.20104	34.79280	34.79185	35.05319
10		31.40	30.74479	30.20459	29.71072	29.27030
20		23.92	23.76072	23.60212	23.43858	23.27201
50		15.46	15.43501	15.41644	15.39646	15.37513
100		11.05	11.04280	11.03948	11.03589	11.03204
500		6.26	6.26202	6.26197	6.26191	6.26185
4	(2, 2)	38.10	35.42569	35.00518	34.99633	35.25319
10		31.69	31.03514	30.48512	29.98168	29.53219
20		24.24	24.08981	23.92873	23.76246	23.59295
50		16.03	16.01226	15.99376	15.97381	15.95249
100		12.28	12.28213	12.27899	12.27557	12.27188
500		12.94	12.97836	12.97832	12.97827	12.97821

$L/h = 5S, \Phi = \pi/3$.

connected with the term $h/(r_0 + h/2)$ through an infinite power series, if using Taylor expansion. Since only finite orders of the term $h/(r_0 + h_0)$ are retained in approximate theories for shells, it would be impossible to give identical results from the theories with different reference surfaces, even if under identical displacement assumptions. However, the difference between the results only has the order of $h/(r_0 + h_0)$ higher than retained. In the limit of flat plates the difference resulting from the latter cause vanishes as $r_0 \to \infty$. See Cheng et al. (1996a, 1997) for perfect interfaces where the lower plane of plates was chosen as the reference plane and Di Sciuva (1992) and Cho and Parmerter (1992, 1993) with the mid-plane being the reference plane.

The interfacial parameters $\bar{R} = 0$, 0.3, 0.6, 0.9 represent a decreasingly stiff interfacial strength, i.e. a progressively weakened bonding. Therefore increasing $\bar{R}$ means relaxation of the interfacial bonding strength, and hence reduction in the overall rigidity of the shell. For the overall elastic response of panels, it is seen from Table 1–6 that due to weakening of the interfacial bond, the rigidity of panels decreases, which leads to increasing central deflection of static bending and decreasing frequencies of flexural vibration, for the same shell configuration. As S decreases the static deflection shown in Tables 1 and 2 for bending problems increases faster with larger values of $\bar{R}$.

To give a better understanding of the way in which local elastic response is affected by progressively weakened interfaces, Figs. 2–8 show, respectively, the variation of dimensionless in-surface displacement,

Table 5
Natural frequencies of a three-ply (90°/0°/90°) laminated circular cylindrical panel

S	Φ	XCL (1995)	$\bar{R}=0$	$\bar{R}=0.3$	$\bar{R}=0.6$	$\bar{R}=0.9$
4	$\pi/3$	12.06	11.99395	10.46062	9.51144	8.90386
10		12.99	12.95592	11.66571	10.57431	9.67627
20		11.25	11.23782	10.76221	10.26312	9.76555
50		8.20	8.20638	8.14615	8.07443	7.99254
100		7.11	7.11737	7.10816	7.09693	7.08374
4	$\pi/2$	5.81	5.78784	5.09342	4.60726	4.26328
10		5.81	5.80312	5.49605	5.20235	4.93480
20		5.42	5.42993	5.36061	5.28276	5.19960
50		6.21	6.22409	6.21946	6.21386	6.20736
100		8.14	8.16500	8.16454	8.16399	8.16333
4	$2\pi/3$	3.36	3.35809	3.13668	2.97307	2.85318
10		4.02	4.02887	3.97886	3.92810	3.87931
20		5.05	5.06662	5.05968	5.05165	5.04278
50		7.62	7.65320	7.65288	7.65248	7.65201
100		10.70	10.74564	10.74561	10.74557	10.74553
4	$5\pi/6$	2.77	2.77869	2.74840	2.72498	2.70721
10		4.15	4.16472	4.16080	4.15662	4.15239
20		5.79	5.81476	5.81432	5.81380	5.81321
50		9.11	9.15694	9.15692	9.15690	9.15687
100		12.88	12.94218	12.94218	12.94217	12.94217

$L/h=5S, m_1=m_2=1$.

bending stress and transverse shear stress distribution through the shell thickness. In practice, the curing process for certain composites is augmented by introducing a very thin adhesive layer in the interfaces in order to reduce the interfacial stresses. Consistently with the foregoing, Fig. 8(a, b) confirms this expectation that the dominant interfacial stress $\bar{\sigma}_{\langle 23\rangle}$, rather than the minor interfacial stress $\bar{\sigma}_{\langle 13\rangle}$ in Fig. 7, decreases significantly as the interfacial parameter increases, especially for small values of S. However, it is also clear from the theoretical prediction that the reduction in dominant interfacial stress $\bar{\sigma}_{\langle 23\rangle}$ is achieved at the expense of increases in overall deflection.

The final example is taken to demonstrate the effect of localized weakness of interfacial bonding. The area of weakly bonding is chosen within a small patch in the range of $\theta^1/L \in [0.3, 0.4]$, and $\theta^2/\Phi \in [0.3, 0.4]$, and the bonding strength is assumed to be uniform as before. A bending problem is considered with the same shell configuration and loading, except the localized interfacial imperfection. Since an exact solution for the problem is impossible, an approximate solution is presented. By means of the Galerkin technique, a solution satisfying the simply supported boundary conditions is assumed in the same form as eqn (C1) in Appendix C. The details of solution are omitted, only central deflection curves in relation to S are given in Fig. 9. Although localized interfacial weakness is far more practical than uniform weakness over entire interfaces, it must be noted that the results shown in Fig. 9 only exhibit qualitative behavior of the shell. This is because we only assume a very simple form of solution using the Galerkin technique. Furthermore, a linearized interfacial model may not be appropriate in practical applications as inconsistency results from the model. Therefore, more sophisticated interfacial models will be necessary to develop new theories.

Table 6
Natural frequencies of a three-ply (90°/0°/90°) laminated circular cylindrical panel

S	E_L/E_T	XCL (1995)	$\bar{R}=0$	$\bar{R}=0.3$	$\bar{R}=0.6$	$\bar{R}=0.9$
4	2	23.78	23.75938	22.09042	20.50491	19.06674
10		17.47	17.47467	17.17775	16.83611	16.46022
20		13.04	13.04730	12.99062	12.92237	12.84323
50		9.18	9.81857	9.81356	9.80744	9.80022
100		9.85	9.85655	9.85592	9.85515	9.85424
4	5	19.70	19.65296	17.52798	15.79736	14.41834
10		16.23	16.22344	15.63297	14.99828	14.34967
20		12.37	12.36674	12.23883	12.08785	11.91707
50		8.99	8.99085	8.97857	8.96360	8.94598
100		8.49	8.49503	8.49338	8.49137	8.48898
4	10	16.29	16.23406	14.14834	12.64254	11.55031
10		15.10	15.09007	14.17882	13.28109	12.43849
20		11.96	11.95545	11.72130	11.45410	11.16326
50		8.61	8.61621	8.59175	8.56208	8.52745
100		7.83	7.84088	7.83744	7.83322	7.82824
4	15	14.32	14.26721	12.37397	11.09644	10.21788
10		14.26	14.24418	13.14101	12.12152	11.21806
20		11.68	11.67951	11.35337	10.99247	10.61252
50		8.43	8.43254	8.39600	8.35194	8.30090
100		7.51	7.51388	7.50856	7.50206	7.49439

$L/h = 5S, \Phi = \pi/3, m_1 = m_2 = 1$.

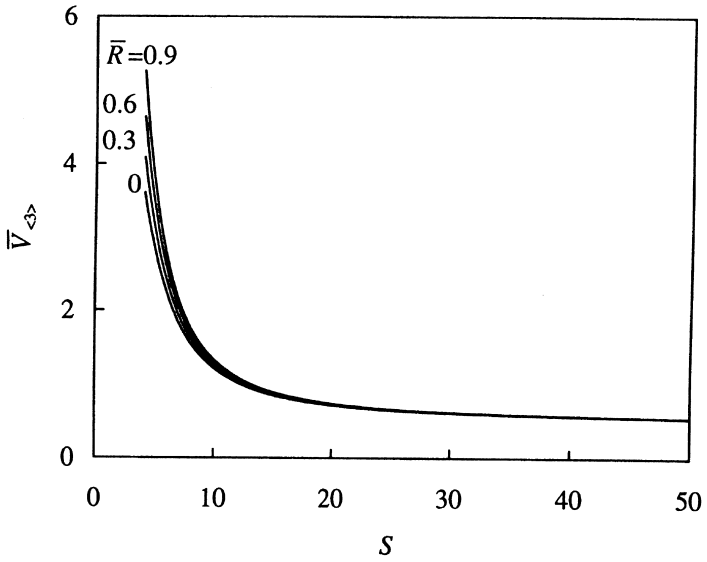

Fig. 9. Central deflection $\bar{V}_{\langle 3\rangle}$ of a three-ply (90°/0°/90°) laminated circular cylindrical panel ($L/h = 4S, \Phi = \pi/4$).

4. Conclusions

This work represents an extension of linear elastodynamic modeling of laminated composite plates (Cheng et al., 1996a) to the case of shells in general configuration, with particular attention paid to the influence of interfacial imperfection. To do this, a spring-layer model as employed in micromechanics is used in a macrostructural analysis environment to model non-uniform and imperfect interfaces of laminated composite shells. The proposed theory has the same advantages as conventional high-order theory. Moreover, it reduces to the zigzag shell theory in the special case of vanishing interface parameters. Numerical results reveal the important feature that interfacial stresses are reduced by weakening the interfacial bonding.

Acknowledgements

The first author is grateful to the National Natural Science Foundation of China for partial financial support.

Appendix A

It is assumed that the transverse normal stress σ^{33} for the shell problem under consideration is negligibly small compared with other stress components, so that it is ignored in the present paper as in most other theories for plates and shells. The displacement model of the shell can be approximately expressed by truncating eqn (1) as

$$v_\alpha(\theta^i;t) = u_\alpha + \psi_\alpha\theta^3 + \varphi_\alpha(\theta^3)^2 + \eta_\alpha(\theta^3)^3 + \sum_{m=1}^{k-1}\left[{}^{(m)}\Delta v_\alpha + {}^{(m)}u_\alpha(\theta^3 - {}^{(m)}h)\right]\mathrm{H}(\theta^3 - {}^{(m)}h),$$

$$v_3(\theta^i;t) = u_3, \tag{A1}$$

where ${}^{(0)}u_i^{(0)}$, ${}^{(0)}u_\alpha^{(1)}$, ${}^{(0)}u_\alpha^{(2)}$, ${}^{(0)}u_\alpha^{(3)}$, ${}^{(m)}u_\alpha^{(0)}$ and ${}^{(m)}u_\alpha^{(1)}$ in eqn (1) have been replaced by the quantities u_i, ψ_α, φ_α, η_α, ${}^{(m)}\Delta v_\alpha$ and ${}^{(m)}u_\alpha$, respectively. Theories developed for calculating separation and slipping delamination need more terms than are retained by eqn (A1) (see Gu and Chattopadhyay, 1996).

The compatibility conditions of transverse shear stresses on both free surfaces of the shell, as well as the interface conditions, are now used to reduce the number of unknowns in eqn (A1). In the absence of tangential tractions on ${}^{(0)}\Omega$ and ${}^{(k)}\Omega$, eqns (A1), (2), (3) and (5), parts one and three, give

$$\psi_\alpha = -u_{3,\alpha} - b_\alpha^\beta u_\beta, \quad \eta_\alpha = d_\alpha^\beta\varphi_\beta + e_\alpha^\beta\sum_{m=1}^{k-1}{}^{(m)}x_\beta, \tag{A2}$$

where, denoting ${}^{(m)}\mu_\omega^\beta = \mu_\omega^\beta|_{({}^{(m)}\Omega)}$ and $(\hat{\mu}^{-1}\beta_\alpha)$ as the inverse of $\hat{\mu}_\alpha^\beta = \mu_\alpha^\beta|_{\theta^3=2h/3}$,

$$d_\alpha^\beta = -\frac{2}{3h}(\hat{\mu}^{-1})_\alpha^\omega\left(\delta_\omega^\beta - \frac{h}{2}b_\omega^\beta\right),\ e_\alpha^\beta = -\frac{1}{3h^2}(\hat{\mu}^{-1})_\alpha^\beta, \quad {}^{(m)}x_\omega = b_\omega^\beta\,{}^{(m)}\Delta v_\beta + {}^{(m)}\mu_\omega^\beta\,{}^{(m)}u_\beta. \tag{A3}$$

The interface condition, the first part of eqn (6), leads to the following $2(k-1)$ linearly algebraic equations involving the $2(k-1)$ unknowns ${}^{(i)}x_\alpha$ $(i = 1,\ldots,k-1)$,

$$\left({}^{(i+1)}E^{\alpha 3\omega 3} - {}^{(i)}E^{\alpha 3\omega 3}\right)\left\{\left[2\delta_{\omega}^{\beta(i)}h - b_{\omega}^{\beta(i)}h^2 + d_{\lambda}^{\beta}\left(3\delta_{\omega}^{\lambda(i)}h^2 - 2b_{\omega}^{\lambda(i)}h^3\right)\right]\varphi_{\beta} + \sum_{m=1}^{i}{}^{(m)}x_{\omega} + e_{\lambda}^{\beta}\left(3\delta_{\omega}^{\lambda(i)}h^2 - 2b_{\omega}^{\lambda(i)}h^3\right)\sum_{m=1}^{k-1}{}^{(m)}x_{\beta}\right\} + {}^{(i)}E^{\alpha 3\omega 3(i)}x_{\omega} = 0,\ (i = 1, \ldots, k-1), \tag{A4}$$

which determine the relationship between ${}^{(i)}x_{\omega}$ and φ_{λ} as

$${}^{(i)}x_{\omega} = {}^{(i)}f_{\omega}^{\lambda}\varphi_{\lambda}, \quad (i = 1, \ldots, k-1). \tag{A5}$$

The interface condition, the second part of eqn (6), and the third part of eqn (A3), give

$${}^{(i)}\Delta v_{\alpha} = {}^{(i)}c_{\alpha}^{\delta}\varphi_{\delta}, \quad {}^{(i)}u_{\alpha} = {}^{(i)}a_{\alpha}^{\delta}\varphi_{\delta}, \quad (i = 1, \ldots, k-1), \tag{A6}$$

where

$${}^{(i)}c_{\alpha}^{\delta} = \left({}^{(i)}\mu^{-1}\right)_{\alpha}^{\rho}{}^{(i)}R_{\rho v}(\theta^{\rho})^{(i+1)}E^{v3\omega 3}\left\{2\delta_{\omega}^{\delta(i)}h - b_{\omega}^{\delta(i)}h^2 + \sum_{m=1}^{i}{}^{(m)}f_{\omega}^{\delta} + \left(3\delta_{\omega}^{\lambda(i)}h^2 - 2b_{\omega}^{\lambda(i)}h^3\right)\left(d_{\lambda}^{\delta} + e_{\lambda}^{\beta}\sum_{m=1}^{k-1}{}^{(m)}f_{\beta}^{\delta}\right)\right\},$$

$${}^{(i)}a_{\alpha}^{\delta} = \left({}^{(i)}\mu^{-1}\right)_{\alpha}^{\omega}\left({}^{(i)}f_{\omega}^{\delta} - b_{\omega}^{\beta}c_{\beta}^{\delta}\right),\ (i = 1, \ldots, k-1). \tag{A7}$$

The coefficients ${}^{(i)}c_{\alpha}^{\delta}$ and ${}^{(i)}a_{\alpha}^{\delta}$ are only related with the interface properties, the material elasticity properties and geometry of laminates.

Substituting eqns (A2) and (A6) into eqn (A1) results in the displacement model of eqn (7), where

$$h_{\alpha}^{\beta} = \delta_{\alpha}^{\beta}\left(\theta^3\right)^2 + \left(d_{\alpha}^{\beta} + e_{\alpha}^{\lambda}\sum_{m=1}^{k-1}{}^{(m)}f_{\lambda}^{\beta}\right)\left(\theta^3\right)^3 + \sum_{m=1}^{k-1}\left[{}^{(m)}c_{\alpha}^{\beta} + {}^{(m)}a_{\alpha}^{\beta}\left(\theta^3 - {}^{(m)}h\right)\right]\mathrm{H}\left(\theta^3 - {}^{(m)}h\right). \tag{A8}$$

Appendix B

By using eqns (7), (2), (3) and (5), eqns (11)–(13) can be rewritten as

$$N^{(1)\alpha} = A^{(1)\alpha\delta}u_{\delta} + B^{(1)\alpha\delta\rho}u_{\delta|\rho} - A^{(1)\alpha 3}u_3 - B^{(2)\alpha\delta\rho}u_{3,\delta\rho} + A^{(2)\alpha\delta}\varphi_{\delta} + B^{(3)\alpha\delta\rho}\varphi_{\delta|\rho},$$

$$N^{(2)\alpha} = A^{(2)\delta\alpha}u_{\delta} + B^{(4)\alpha\delta\rho}u_{\delta|\rho} - A^{(2)\alpha 3}u_3 - B^{(5)\alpha\delta\rho}u_{3,\delta\rho} + A^{(3)\alpha\delta}\varphi_{\delta} + B^{(6)\alpha\delta\rho}\varphi_{\delta|\rho},$$

$$N^{(3)\alpha} = A^{(4)\alpha\delta}\varphi_{\delta},$$

$$N^{(1)3} = A^{(1)\delta 3}u_\delta + B^{(1)\delta\rho 3}u_{\delta|\rho} - A^{(1)33}u_3 - B^{(2)\delta\rho 3}u_{3,\delta\rho} + A^{(2)\delta 3}\varphi_\delta + B^{(3)\delta\rho 3}\varphi_{\delta|\rho},$$

$$M^{(1)\alpha\beta} = B^{(1)\delta\alpha\beta}u_\delta + C^{(1)\alpha\beta\delta\rho}u_{\delta|\rho} - B^{(1)\alpha\beta 3}u_3 - C^{(2)\alpha\beta\delta\rho}u_{3,\delta\rho} + B^{(4)\delta\alpha\beta}\varphi_\delta + C^{(3)\alpha\beta\delta\rho}\varphi_{\delta|\rho},$$

$$M^{(2)\alpha\beta} = B^{(2)\delta\alpha\beta}u_\delta + C^{(2)\delta\rho\alpha\beta}u_{\delta|\rho} - B^{(2)\alpha\beta 3}u_3 - C^{(4)\alpha\beta\delta\rho}u_{3,\delta\rho} + B^{(5)\delta\alpha\beta}\varphi_\delta + C^{(5)\alpha\beta\delta\rho}\varphi_{\delta|\rho},$$

$$M^{(3)\alpha\beta} = B^{(3)\delta\alpha\beta}u_\delta + C^{(3)\delta\rho\alpha\beta}u_{\delta|\rho} - B^{(3)\alpha\beta 3}u_3 - C^{(5)\delta\rho\alpha\beta}u_{3,\delta\rho} + B^{(6)\delta\alpha\beta}\varphi_\delta + C^{(6)\alpha\beta\delta\rho}\varphi_{\delta|\rho}. \tag{B1}$$

Substituting the resulting expressions into eqn (9) then yields the displacement-based field equations as

$$-\left(A^{(1)\alpha\delta} - B^{(1)\delta\alpha\beta}_{|\beta}\right)u_\delta + \left(B^{(1)\delta\alpha\rho} - B^{(1)\alpha\delta\rho} + C^{(1)\alpha\beta\delta\rho}_{|\beta}\right)u_{\delta|\rho} + C^{(1)\alpha\beta\delta\rho}u_{\delta|\rho\beta}$$

$$+\left(A^{(1)\alpha 3} - B^{(1)\alpha\beta 3}_{|\beta}\right)u_3 - \left(B^{(1)\alpha\rho 3}u_{3,\rho} + B^{(2)\alpha\delta\rho} - C^{(2)\alpha\beta\delta\rho}_{|\beta}\right)u_{3,\delta\rho} - C^{(2)\alpha\beta\delta\rho}u_{3,\delta\rho\beta}$$

$$-\left(A^{(2)\alpha\delta} - B^{(4)\delta\alpha\beta}_{|\beta}\right)\varphi_\delta - \left(B^{(3)\alpha\delta\rho} - B^{(4)\delta\alpha\rho} - C^{(3)\alpha\beta\delta\rho}_{|\beta}\right)\varphi_{\delta|\rho} + C^{(3)\alpha\beta\delta\rho}\varphi_{\delta|\rho\beta}$$

$$-I^{(1)\beta\alpha}\ddot{u}_\beta + I^{(2)\beta\alpha}\ddot{u}_{3,\beta} - I^{(3)\beta\alpha}\ddot{\varphi}_\beta = 0,$$

$$\left(A^{(1)\delta 3} + B^{(2)\delta\alpha\beta}_{|\alpha\beta}\right)u_\delta + \left(B^{(1)\delta\rho 3} + B^{(2)\delta\rho\beta}_{|\beta} + B^{(2)\delta\alpha\rho}_{|\alpha} + C^{(2)\delta\rho\alpha\beta}_{|\alpha\beta}\right)u_{\delta|\rho}$$

$$+\left(B^{(2)\delta\alpha\rho} + C^{(2)\delta\rho\alpha\beta}_{|\beta} + C^{(2)\delta\rho\beta\alpha}_{|\beta}\right)u_{\delta|\rho\alpha} + C^{(2)\delta\rho\alpha\beta}u_{\delta|\rho\alpha\beta}$$

$$-\left(A^{(1)33} + B^{(2)\alpha\beta 3}_{|\alpha\beta}\right)u_3 - \left(B^{(2)\rho\beta 3}_{|\beta} + B^{(2)\alpha\rho 3}_{|\alpha}\right)u_{3,\rho}$$

$$-\left(2B^{(2)\delta\rho 3} + C^{(4)\alpha\beta\delta\rho}_{|\alpha\beta}\right)u_{3,\delta\rho} - \left(C^{(4)\alpha\beta\delta\rho}_{|\beta} + C^{(4)\beta\alpha\delta\rho}_{|\beta}\right)u_{3,\delta\rho\alpha} - C^{(4)\alpha\beta\delta\rho}u_{3,\alpha\beta\delta\rho}$$

$$+\left(A^{(2)\delta 3} + B^{(5)\delta\alpha\beta}_{|\alpha\beta}\right)\varphi_\delta + \left(B^{(3)\delta\rho 3} + B^{(5)\delta\alpha\rho}_{|\alpha} + B^{(5)\delta\rho\beta}_{|\beta} + C^{(5)\alpha\beta\delta\rho}_{|\alpha\beta}\right)\varphi_{\delta|\rho}$$

$$+\left(B^{(5)\delta\alpha\rho} + C^{(5)\alpha\beta\delta\rho}_{|\beta} + C^{(5)\beta\alpha\delta\rho}_{|\beta}\right)\varphi_{\delta|\rho\alpha} + C^{(5)\alpha\beta\delta\rho}\varphi_{\delta|\rho\alpha\beta}$$

$$+P^3 - I^{(1)33}\ddot{u}_3 - \left(I^{(2)\beta\alpha}\ddot{u}_\alpha\right)_{|\beta} + \left(I^{(4)\alpha\beta}\ddot{u}_{3,\alpha}\right)_{|\beta} - \left(I^{(6)\alpha\beta}\ddot{\varphi}_\alpha\right)_{|\beta} = 0,$$

$$-\left(A^{(2)\delta\alpha} - B^{(3)\delta\alpha\beta}_{|\beta}\right)u_\delta + \left(B^{(3)\delta\alpha\rho} - B^{(4)\alpha\delta\rho} + C^{(3)\delta\rho\alpha\beta}_{|\beta}\right)u_{\delta|\rho} + C^{(3)\delta\rho\alpha\beta}u_{\delta|\rho\beta}$$

$$+\left(A^{(2)\alpha 3}-B^{(3)\alpha\beta 3}_{|\beta}\right)u_3-B^{(3)\alpha\rho 3}u_{3,\rho}+\left(B^{(5)\alpha\delta\rho}-C^{(5)\delta\rho\alpha\beta}_{|\beta}\right)u_{3,\delta\rho}-C^{(5)\delta\rho\alpha\beta}u_{3,\delta\rho\beta}$$

$$-\left(A^{(3)\alpha\delta}+A^{(4)\alpha\delta}-B^{(6)\delta\alpha\beta}_{|\beta}\right)\varphi_\delta+\left(B^{(6)\delta\alpha\rho}-B^{(6)\alpha\delta\rho}+C^{(6)\alpha\beta\delta\rho}_{|\beta}\right)\varphi_{\delta|\rho}+C^{(6)\alpha\beta\delta\rho}\varphi_{\delta|\rho\beta}$$

$$-I^{(3)\alpha\beta}\ddot{u}_\beta+I^{(6)\alpha\beta}\ddot{u}_{3,\beta}-I^{(5)\beta\alpha}\ddot{\varphi}_\beta=0, \tag{B2}$$

where

$$\left[A^{(1)\alpha\delta},\,A^{(2)\alpha\delta},\,A^{(3)\alpha\delta}\right]=\int_0^h H^{\lambda\beta\omega\rho}\mu^\sigma_\omega\mu^\nu_\lambda\left[\mu^\alpha_{\nu|\beta}\mu^\delta_{\sigma|\rho},\,\mu^\alpha_{\nu|\beta}h^\delta_{\sigma|\rho},\,h^\alpha_{\nu|\beta}h^\delta_{\sigma|\rho}\right]\mu\,\mathrm{d}\theta^3,$$

$$A^{(4)\alpha\delta}=\int_0^h E^{\lambda 3\omega 3}\left(\mu^\sigma_\omega h^\delta_{\sigma,3}+b^\sigma_\omega h^\delta_\sigma\right)\left(\mu^\nu_\lambda h^\alpha_{\nu,3}+b^\nu_\lambda h^\alpha_\nu\right)\mu\,\mathrm{d}\theta^3,$$

$$\left[A^{(1)\alpha 3},\,A^{(2)\alpha 3},\,A^{(1)33}\right]=\int_0^h H^{\lambda\beta\omega\rho}\mu^\sigma_\omega\mu^\nu_\lambda b_{\sigma\rho}\left[\mu^\alpha_{\nu|\beta},\,h^\alpha_{\nu|\beta},\,b_{\nu\beta}\right]\mu\,\mathrm{d}\theta^3,$$

$$\left[B^{(1)\alpha\delta\rho},\,B^{(2)\alpha\delta\rho},\,B^{(3)\alpha\delta\rho},\,B^{(4)\alpha\delta\rho},\,B^{(5)\alpha\delta\rho},\,B^{(6)\alpha\delta\rho}\right]$$

$$=\int_0^h H^{\lambda\beta\omega\rho}\mu^\sigma_\omega\mu^\nu_\lambda\left[\mu^\alpha_{\nu|\beta}\mu^\delta_\sigma,\,\theta^3\mu^\alpha_{\nu|\beta}\delta^\delta_\sigma,\,\mu^\alpha_{\nu|\beta}h^\delta_\sigma,\,h^\alpha_{\nu|\beta}\mu^\delta_\sigma,\,\theta^3h^\alpha_{\nu|\beta}\delta^\delta_\sigma,\,h^\alpha_{\nu|\beta}h^\alpha_\sigma\right]\mu\,\mathrm{d}\theta^3,$$

$$\left[B^{(1)\alpha\beta 3},\,B^{(2)\alpha\beta 3},\,B^{(3)\alpha\beta 3}\right]=\int_0^h H^{\lambda\beta\omega\rho}\mu^\sigma_\omega\mu^\nu_\lambda b_{\sigma\rho}\left[\mu^\alpha_\nu,\,\theta^3\delta^\alpha_\nu,\,h^\alpha_\nu\right]\mu\,\mathrm{d}\theta^3,$$

$$\left[C^{(1)\alpha\beta\delta\rho},\,C^{(2)\alpha\beta\delta\rho},\,C^{(3)\alpha\beta\delta\rho},\,C^{(4)\alpha\beta\delta\rho},\,C^{(5)\alpha\beta\delta\rho},\,C^{(6)\alpha\beta\delta\rho}\right]$$

$$=\int_0^h H^{\lambda\beta\omega\rho}\mu^\sigma_\omega\mu^\nu_\lambda\left[\mu^\alpha_\nu\mu^\delta_\sigma,\,\theta^3\mu^\alpha_\nu\delta^\delta_\sigma,\,\mu^\alpha_\nu h^\delta_\sigma,\left(\theta^3\right)^2\delta^\alpha_\nu\delta^\delta_\sigma,\,\theta^3\delta^\alpha_\nu h^\delta_\sigma,\,h^\alpha_\nu h^\delta_\sigma\right]\mu\,\mathrm{d}\theta^3. \tag{B3}$$

Appendix C

Exact closed-form solutions to the example of Section 3 can be found by assuming the following form

$$[u_1,\,\varphi_1]=[U_1,\,\Phi_1]\cos\frac{m_1\pi\theta^1}{L}\,\sin\frac{m_2\pi\theta^2}{\Phi}\mathrm{e}^{i\omega t},$$

$$[u_2,\,\varphi_2]=[U_2,\,\Phi_2]\sin\frac{m_1\pi\theta^1}{L}\,\cos\frac{m_2\pi\theta^2}{\Phi}\mathrm{e}^{i\omega t},$$

$$u_3 = U_3 \sin\frac{m_1\pi\theta^1}{L} \sin\frac{m_2\pi\theta^2}{\Phi} e^{i\omega t}, \tag{C1}$$

which yields, after substituting eqn (C1) into eqn (B2),

$$\mathbf{AX} = \mathbf{F}, \tag{C2}$$

where

$$\mathbf{X} = [U_1 \;\; U_2 \;\; U_3 \;\; \Phi_1 \;\; \Phi_2]^T, \quad \mathbf{F} = [0 \;\; 0 \;\; -p_0 \;\; 0 \;\; 0]^T, \tag{C3}$$

and $\mathbf{A}$ is a 5×5 symmetric matrix ($A_{IJ} = A_{JI}$, $I, J = 1, \ldots, 5$) where its elements, expressed in terms of $l_1 = m_1\pi/L$ and $l_2 = m_2\pi/\Phi$, are

$$A_{11} = -l_1^2 C^{(1)1111} - l_2^2 C^{(1)1212} + I^{(1)11}\omega^2,$$

$$A_{12} = -l_1 l_2 \left(C^{(1)1122} + C^{(1)1221}\right),$$

$$A_{13} = -l_1 B^{(1)113} + l_1^3 C^{(2)1111} + l_1 l_2^2 \left(C^{(2)1122} + C^{(2)1212} + C^{(2)1221}\right) - l_1 I^{(2)11}\omega^2,$$

$$A_{14} = -l_1^2 C^{(3)1111} - l_2^2 C^{(3)1212} + I^{(3)11}\omega^2,$$

$$A_{15} = -l_1 l_2 \left(C^{(3)1122} + C^{(3)1221}\right),$$

$$A_{22} = -l_2^2 C^{(1)2222} - l_1^2 C^{(1)2121} + I^{(1)22}\omega^2,$$

$$A_{23} = -l_2 B^{(1)223} + l_1^2 l_2 C^{(2)2211} + l_2^3 C^{(2)2222} + l_1^2 l_2 \left(C^{(2)2112} + C^{(2)2121}\right) - l_2 I^{(2)22}\omega^2,$$

$$A_{24} = -l_1 l_2 \left(C^{(3)2211} + C^{(3)2112}\right),$$

$$A_{25} = -l_2^2 C^{(3)2222} - l_1^2 C^{(3)2121} + I^{(3)22}\omega^2,$$

$$A_{33} = -A^{(1)33} + 2l_1^2 B^{(2)113} + 2l_2^2 B^{(2)223} - l_1^4 C^{(4)1111} - l_1^2 l_2^2 \left(C^{(4)1122} + C^{(4)2211}\right) - l_2^4 C^{(4)2222}$$
$$- l_1^2 l_2^2 \left(C^{(4)1212} + C^{(4)1221} + C^{(4)2112} + C^{(4)2121}\right) + \left(I^{(1)33} + l_1^2 I^{(4)11} + l_2^2 I^{(4)22}\right)\omega^2,$$

$$A_{34} = -l_1 B^{(3)113} + l_1^3 C^{(5)1111} + l_1 l_2^2 \left(C^{(5)2211} + C^{(5)1212} + C^{(5)2112}\right) - l_1 I^{(6)11}\omega^2,$$

$$A_{35} = -l_2 B^{(3)223} + l_1^2 l_2 C^{(5)1122} + l_2^3 C^{(5)2222} + l_1^2 l_2 \left(C^{(5)1221} + C^{(5)2121}\right) - l_2 I^{(6)22}\omega^2,$$

$$A_{44} = -A^{(4)11} - l_1^2 C^{(6)1111} - l_2^2 C^{(6)1212} + I^{(5)11}\omega^2,$$

$$A_{45} = -l_1 l_2 \left(C^{(6)1122} + C^{(6)1221} \right),$$

$$A_{55} = -A^{(4)22} - l_2^2 C^{(6)2222} - l_1^2 C^{(6)2121} + I^{(5)22}\omega^2. \tag{C4}$$

References

Aboudi, J., 1987. Damage in composites—modelling of imperfect bonding. Compos. Sci. Tech. 28, 103–128.

Achenbach, J.D., Zhu, H., 1989. Effect of interfacial zone on mechanical behaviour and failure of fibre-reinforced composites. J. Mech. Phys. Solids 37, 381–393.

Benveniste, Y., Dvorak, G.J., 1990. On a correspondence between mechanical and thermal fields with slipping interfaces. In: Dvorak, G.J. (Ed.), Inelastic Deformation of Composite Materials, Proceedings of IUTAM Symposium. Springer-Verlag, New York, pp. 77–98.

Cheng, Z.Q., Howson, W.P., Williams, F.W., 1997. Modelling of weakly bonded laminated composite plates at large deflections. Int. J. Solids Structures 34, 3583–3599.

Cheng, Z.Q., Jemah, A.K., Williams, F.W., 1996a. Theory for multilayered anisotropic plates with weakened interfaces. J. Appl. Mech. 63, 1019–1026.

Cheng, Z.Q., Kennedy, D., Williams, F.W., 1996b. Effect of interfacial imperfection on buckling and bending behavior of composite laminates. AIAA J. 34, 2590–2595.

Cheng, Z.Q., Kitipornchai, S., 1998. Nonlinear theory for composite laminated shells with interfacial damage. J. Appl. Mech. 65, 711–718.

Cho, M., Parmerter, R.R., 1992. An efficient higher-order plate theory for laminated composites. Compos. Struct. 20, 113–123.

Cho, M., Parmerter, R.R., 1993. Efficient higher order composite plate theory for general lamination configurations. AIAA J. 31, 1299–1306.

Crawley, E.F., de Luis, J., 1987. Use of piezoelectric actuators as elements of intelligent structures. AIAA J. 25, 1373–1385.

Di Sciuva, M., 1992. Multilayered anisotropic plate models with continuous interlaminar stresses. Compos. Struct. 22, 149–167.

Di Sciuva, M., Icardi, U., 1993. Discrete-layer models for multilayered shells accounting for interlayer continuity. Meccanica 28, 281–291.

Gu, H.Z., Chattopadhyay, A., 1996. Delamination buckling and postbuckling of composite cylindrical shells. AIAA J. 34, 1279–1286.

Hashin, Z., 1990. Thermoelastic properties of fibre composites with imperfect interface. Mech. Mater. 8, 333–348.

Hashin, Z., 1991. Thermoelastic properties of particulate composites with imperfect interface. J. Mech. Phys. Solids 39, 745–762.

He, L.H., 1994. A linear theory of laminated shells accounting for continuity of displacements and transverse shear stresses at layer interfaces. Int. J. Solids Structures 31, 613–627.

He, L.H., 1995. Non-linear theory of laminated shells accounting for continuity conditions of displacements and tractions at layer interfaces. Int. J. Mech. Sci. 37, 161–173.

Lai, Y.S., Wang, C.Y., Tien, Y.M., 1997. Micromechanical analysis of imperfectly bonded layered media. J. Engng Mech. 123, 986–995.

Lee, K.H., Cao, L., 1996. A predictor-corrector zigzag model for the bending of laminated composite plates. Int. J. Solids Structures 33, 879–897.

Librescu, L., 1975. Elastostatistics and Kinetics of Anisotropic and Heterogeneous Shell-type Structures. Noordhoff, Leyden.

Librescu, L., Schmidt, R., 1991. Substantiation of a shear-deformable theory of anisotropic composite laminated shells accounting for the interlaminar continuity conditions. Int. J. Engng Sci. 29, 669–683.

Naghdi, P.M., 1963. Foundation of elastic shell theory. In: Sneddon, I.N., Hill, R. (Eds.), Progress of Solid Mechanics, vol. 4. Amsterdam, North-Holland.

Noor, A.K., Burton, W.S., 1990. Assessment of computational models for multilayered composite shells. Appl. Mech. Rev. 43, 67–97.

Noor, A.K., Peters, J.M., 1989. A posteriori estimates for shear correction factors in multilayered composite cylinders. J. Engng Mech. 115, 1225–1244.

Qu, J., 1993a. Eshelby tensor for an elastic inclusion with slightly weakened interfaces. J. Appl. Mech. 60, 1048–1050.

Qu, J., 1993b. The effect of slightly weakened interfaces on the overall elastic properties of composite materials. Mech. Mater. 14, 269–281.

Reddy, J.N., 1997. Mechanics of Laminated Composite Plates: Theory and Analysis. CRC Press, Boca Raton, Florida.

Reddy, J.N., Robbins Jr, D.H., 1994. Theories and computational models for composite laminates. Appl. Mech. Rev. 47, 147–169.

Schmidt, R., Librescu, L., 1994. Further results concerning the refined theory of anisotropic laminated composite plates. J. Engng Math. 28, 407–425.

Schmidt, R., Librescu, L., 1996. Geometrically nonlinear theory of laminated anisotropic composite plates featuring interlayer slips. Nova J. Math. Game Theory Algebra 5, 131–147.

Toledano, A., Murakami, H., 1988. Shear deformable two-layer plate theory with interlayer slip. J. Engng Mech. 114, 604–623.

Varadan, T.K., Bhaskar, K., 1991. Bending of laminated orthotropic cylindrical shells—An elasticity approach. Compos. Struct. 17, 141–156.

Xavier, P.B., Chew, C.H., Lee, K.H., 1995. Buckling and vibration of multilayer orthotropic composite shells using a simple higher-order layerwise theory. Int. J. Solids Structures 32, 3479–3497.

Xavier, P.B., Lee, K.H., Chew, C.H., 1993. An improved zigzag model for the bending of laminated composite shells. Compos. Struct. 26, 123–138.

Zhong, Z., Meguid, S.A., 1996. On the eigenstrain problem of a spherical inclusion with an imperfectly bonded interface. J. Appl. Mech. 63, 877–883.